IEEE Access
Multidisciplinary | Rapid Review | Open Access Journal

Received December 30, 2019, accepted January 10, 2020, date of publication January 15, 2020, date of current version January 27, 2020.

Digital Object Identifier 10.1109/ACCESS.2020.2966719

Recursive Least-Squares Lattice Algorithm Combined With Secondary-Path Innovation and Lattice-Order Decision Algorithms for Active Noise Control

DONG WOO KIM AND POOGYEON PARK, (Member, IEEE)
Department of Electronic and Electrical Engineering, Pohang University of Science and Technology, Pohang 37673, South Korea

Corresponding author: Poogyeon Park (ppg@postech.ac.kr)

This work was supported by the National Research Foundation of Korea (NRF) Grant through the Korea Government (MSIT) under Grant 2019R1A4A1029003.

ABSTRACT This paper proposes a new active noise control (ANC) system based on a recursive least-squares lattice (RLSL) algorithm by designing secondary-path innovation (SPI) and lattice-order decision (LOD) algorithms. The SPI algorithm associated with the power spectral factorization of the secondary path is designed to apply the RLSL algorithm to the ANC system without the filtered-input structure. The SPI algorithm whitens the error microphone signals into the *virtual* error signals just ahead of the secondary path to construct the *virtual* desired signals corresponding to the outputs of the lattice filter. The LOD algorithm is designed to operate the ANC system without knowing the tap length of the optimal finite impulse response (FIR) filter. The decision algorithm using the initial and final estimation errors of the lattice filter estimates the tap length of the optimal FIR filter by increasing the lattice order one-by-one until the final estimation error reaches below a threshold value. Even in environments where the tap length of the optimal FIR filter is unknown, the proposed ANC system with low computational complexity shows almost the same performance as the ANC system based on a filtered-input recursive least squares algorithm.

INDEX TERMS Active noise control, lattice-order decision algorithm, recursive least-squares lattice algorithm, secondary-path innovation algorithm, *virtual* error signals.

I. INTRODUCTION

Active noise control (ANC) systems suppress noises using destructive interference signals. Various adaptive filtering algorithms have been applied to ANC systems [1]. Among them, the filtered-input least mean square (FxLMS) algorithm is widely used owing to its simple structure for implementation in ANC systems [2], [3]. However, the FxLMS algorithm uses a fixed step-size, which causes a trade-off between convergence rate and steady-state error level. To mitigate the drawback, various variable step-size FxLMS (VSS-FxLMS) algorithms have been introduced [4]–[6]. VSS-FxLMS algorithms provide faster convergence rate and better performance for noise reduction than the FxLMS algorithm. However, the performance of VSS-FxLMS algorithms based on a stochastic gradient approach is degraded for correlated inputs [7]. The filtered-input affine projection (FxAP) algorithm has been proposed to handle the difficulty with correlated inputs [8]–[10]. This algorithm shows better performance for correlated inputs, but its computational complexity is too high for implementation in an ANC system. Especially matrix inversion should be obtained through VSS-FxAP algorithms [10]. The filtered-input gradient adaptive lattice (FxGAL) algorithm has been proposed to reduce the computational complexity and improve the performance degradation with correlated inputs [11]–[17]. The FxGAL algorithm using the lattice form to orthogonalize correlated inputs shows better performance and lower computational complexity than the FxAP algorithm. However, as the regression coefficients are updated by a stochastic gradient approach such as the normalized least mean square (NLMS) algorithm, the performance of the FxGAL algorithm cannot reach that of the filtered-input recursive least-squares (FxRLS) algorithm based on a least-square

The associate editor coordinating the review of this manuscript and approving it for publication was Mohammad Zia Ur Rahman.

estimation [18]–[21]. Although the FxRLS algorithm shows the best performance among all aforementioned algorithms, it has not been applied to ANC systems owing to its high computational complexity of $O(M^2)$ operations per iteration [22], where M is the tap length of the filter. A recursive least-squares lattice (RLSL) algorithm is expected to be the best alternative to solve this problem [23], [24]. The RLSL algorithm has many advantages such as fast convergence rate, low computational complexity, and robustness for correlated inputs. However, it has not been generally used in ANC systems with a filtered-input structure because of its nonlinear property and the computational complexity of the filtered-input structure [25].

This paper proposes the secondary-path innovation (SPI) algorithm to overcome the limitation of the filtered-input structure in ANC systems. The SPI algorithm associated with the power spectral factorization of the secondary path whitens the error microphone signals into the *virtual* error signals just ahead of the secondary path to construct *virtual* desired signals corresponding to the outputs of the lattice filter. In addition, this paper proposes the lattice-order decision (LOD) algorithm. This algorithm uses the initial and final estimation errors to decide the order of the lattice filters considering excess ratio of lattice order (*ERLO*) and the performance for noise reduction. The proposed ANC system with low computational complexity shows almost the same performance as the ANC system based on the FxRLS algorithm. Moreover, while the conventional ANC systems can be only operated by knowing the tap length of the optimal finite impulse response (FIR) filter in the primary path, the proposed ANC system can cancel the noise effectively without knowing the tap length of the optimal FIR filter.

The rest of this paper is organized as follows. In section II, the RLSL algorithm is introduced and applied to the ANC system. In section III, the SPI and LOD algorithms are proposed. Simulation results are shown in section IV, and conclusion is presented in section V.

II. PRELIMINARY

The desired signals to be reduced are expressed as

$$d(k) = \mathbf{p}(z)x(k) + v(k), \tag{1}$$

where $\mathbf{p}(z)$ is the transfer function from the reference sensor to the error microphone sensor. $x(k)$ represents the input noise signals, and $v(k)$ represents the measurement noise signals.

In the lattice filter, order-update recursions for forward and backward prediction errors are defined as

$$f_m(k) = f_{m-1}(k) + \Gamma_{f,m}(k-1)b_{m-1}(k-1), \tag{2}$$
$$b_m(k) = b_{m-1}(k-1) + \Gamma_{b,m}(k-1)f_{m-1}(k), \tag{3}$$

where $m = 1, 2, \ldots, M$ and M is the lattice order. $f_0(k)$ and $b_0(k)$ are set to $x(k)$. $f_m(k)$ and $b_m(k)$ represent the forward and backward prediction errors, respectively. $\Gamma_{f,m}(k)$ and $\Gamma_{b,m}(k)$ represent the forward and backward reflection coefficient, respectively. The output signals of the lattice filter

Algorithm 1 RLSL Algorithm [26]

Predictions: Starting with $k = 1$, calculate the order updates in the sequence $m = 1, 2, \ldots M$:

$$\begin{aligned}
\Delta_{m-1}(k) &= \lambda\Delta_{m-1}(k-1) + \gamma_{m-1}(k-1)b_{m-1}(k-1)f_{m-1}(k),\\
F_{m-1}(k) &= \lambda F_{m-1}(k-1) + \gamma_{m-1}(k-1)|f_{m-1}(k)|^2,\\
B_{m-1}(k) &= \lambda B_{m-1}(k-1) + \gamma_{m-1}(k)|b_{m-1}(k)|^2,\\
\Gamma_{f,m}(k) &= -\frac{\Delta_{m-1}(k)}{B_{m-1}(k-1)},\\
\Gamma_{b,m}(k) &= -\frac{\Delta_{m-1}(k)}{F_{m-1}(k)},\\
\gamma_m(k) &= \gamma_{m-1}(k) - \frac{\gamma_{m-1}(k)^2|b_{m-1}(k)|^2}{B_{m-1}(k)},
\end{aligned}$$

where $\lambda = [0.9, 1]$.

Filtering: For $k = 1, 2, \ldots$, calculate the order updates in the sequence $m = 0, 1, \ldots M$:

$$\begin{aligned}
\rho_m(k) &= \lambda\rho_m(k-1) + \gamma_m(k)b_m(k)\epsilon_m(k),\\
\epsilon_{m+1}(k) &= \epsilon_m(k-1) - \kappa_m(k-1)b_m(k),\\
\kappa_m(k) &= \frac{\rho_m(k)}{B_m(k)}.
\end{aligned}$$

Initialization at time $k = 0$:

$$\begin{aligned}
&\Delta_{m-1}(0) = 0, \quad F_{m-1}(0) = B_{m-1}(0) = \delta,\\
&\Gamma_{f,m}(0) = \Gamma_{b,m}(0) = 0, \quad \gamma_0(0) = \sigma_v(k)^2, \quad \rho_m(0) = 0,
\end{aligned}$$

where δ is very small value. $\sigma_v(k)^2$ is the variance of the measurement noises $v(k)$ and is approximated as

$$\begin{aligned}
\sigma_e(k)^2 &\approx \zeta\sigma_e(k)^2 + (1-\zeta)e(k)^2,\\
\sigma_v(k)^2 &\approx 0.005\sigma_e(k)^2,
\end{aligned}$$

where ζ was set to 0.999.

Initialization at the zeroth-order:

$$\begin{aligned}
&f_0(k) = b_0(k) = x(k), \quad F_0(k) = B_0(k) = \lambda F_0(k-1) + |x(k)|^2,\\
&\gamma_0(k) = \sigma_v(k)^2, \quad \epsilon_0(k) = \hat{d}_r(k)
\end{aligned}$$

where $\hat{d}_r(k)$ is generated by the proposed SPI algorithm.

are defined as

$$y_r(k) = \sum_{m=0}^{M} b_m(k)\kappa_m(k), \tag{4}$$

where $\kappa_m(k)$ represents the regression coefficient and is updated by the RLSL algorithm. The update rule of the RLSL algorithm was proposed by [26] and is shown in Algorithm 1. The output signals through the secondary path are defined as

$$y(k) = \sum_{i=0}^{N} y_r(k-i)h_i = \mathbf{y}_r^T(k)\mathbf{h}_o, \tag{5}$$

where the secondary-path (SP) model tap $\mathbf{h_o}$ is in $R^{N\times 1}$, and the vector of the output signals before passing the SP model $\mathbf{y}_r(k)$ is denoted by $[y_r(k)y_r(k-1)\cdots y_r(k-N+1)]^T \in R^{N\times 1}$.

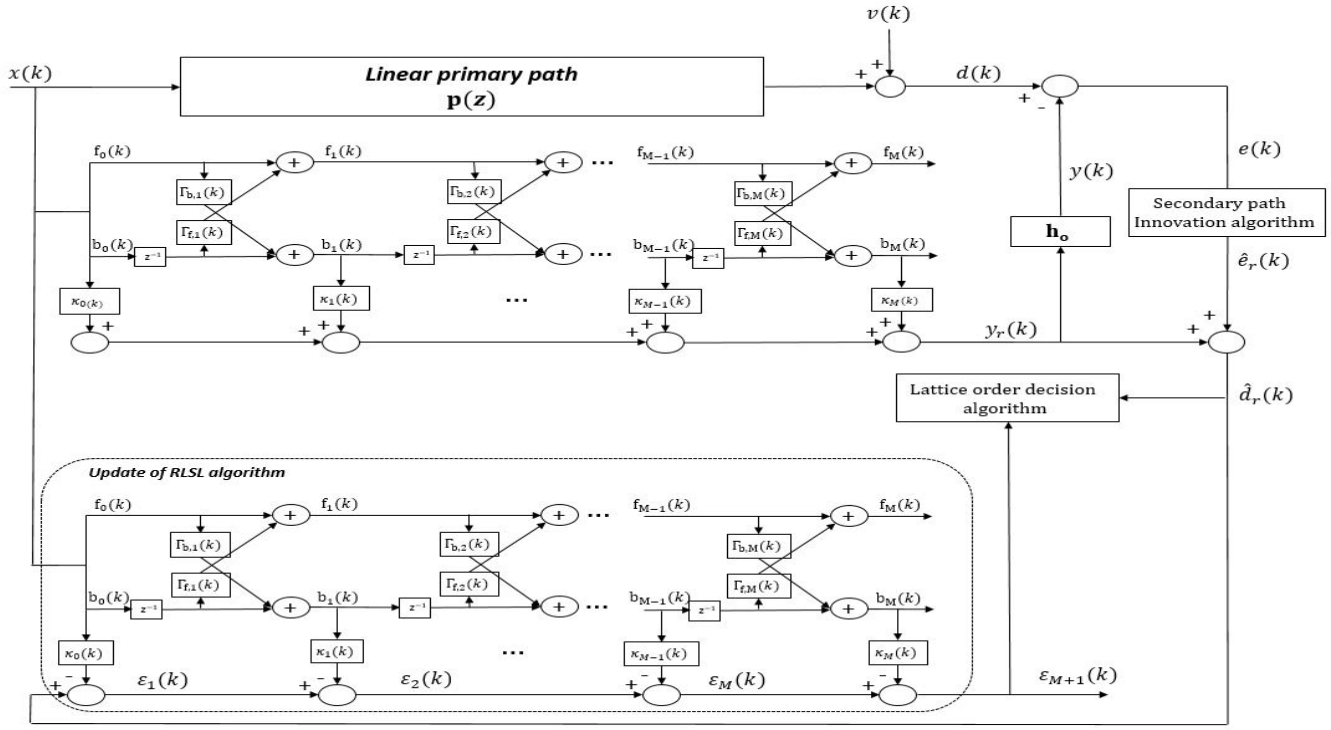

FIGURE 1. Proposed RLSL ANC system.

The error microphone signals $e(k)$ that can be observed are defined as

$$e(k) = d(k) - y(k). \tag{6}$$

As the signals $e(k)$ are distorted by the secondary path, the *virtual* desired signals $\hat{d}_r(k)$ corresponding to the outputs of the lattice filter, which is required to apply the RLSL algorithm to the ANC system without the filtered-input structure, cannot be obtained using $e(k)$. The *virtual* desired signals are estimated using the proposed method in section III.

III. PROPOSED METHOD

The RLSL algorithm with low computational complexity has a fast convergence rate and robustness for correlated inputs in environments where the tap length of the optimal FIR filter is unknown. However, the ANC systems with the secondary path generally do not use the RLSL algorithm, as it is not easy to apply this algorithm to the filtered-input structure. In this paper, for applying the RLSL algorithm to the ANC systems without the filtered-input structure, the SPI algorithm is proposed.

A. SECONDARY-PATH INNOVATION ALGORITHM

The secondary path is modeled with the FIR filters of length N as follows.

$$H_o(z) = h_0 + h_1 z^{-1} + h_2 z^{-2} + \cdots + h_{N-1} z^{-N+1}. \tag{7}$$

The error microphone signals $e(k)$ can be rewritten as

$$\begin{aligned} e(k) &= d(k) - y(k), && (8)\\ &= \mathbf{d}_r(k)^T \mathbf{h_o} + v(k) - \mathbf{y}_r(k)^T \mathbf{h_o}, && (9)\\ &= \{\mathbf{d}_r(k) - \mathbf{y}_r(k)\}^T \mathbf{h_o} + v(k), && (10)\\ &= \mathbf{e}_r(k)^T \mathbf{h_o} + v(k), && (11)\\ &= \sum_{n=0}^{N-1} e_r(k-n) h_n + v(k), && (12) \end{aligned}$$

where $\mathbf{d}_r(k) \in \mathcal{R}^{N\times 1}$ and $\mathbf{e}_r(k) \in \mathcal{R}^{N\times 1}$ represent the vector of the *virtual* desired signals and the *virtual* error signals corresponding to the outputs of the lattice filter just ahead of the secondary path, respectively.

The equation (12) can be rewritten in the form of state-space representation as

$$\begin{aligned} \mathbf{e}_{r,pri}(k+1) &= A\mathbf{e}_{r,pri}(k) + Be_r(k),\\ e(k) &= C\mathbf{e}_{r,pri}(k) + De_r(k) + v(k), \end{aligned} \tag{13}$$

where $\mathbf{e}_{r,pri}(k) = [e_r(k-1)\ \ e_r(k-2)\cdots e_r(k-N+1)]^T \in \mathcal{R}^{(N-1)\times 1}$ represents the state vector stacking the *prior virtual* error signals. A, B, C, and D are defined as

$$A = \begin{bmatrix} \mathbf{0} & 0 \\ \mathbf{I} & 0 \end{bmatrix} \in \mathcal{R}^{(N-1)\times(N-1)}, \quad B = [1\ \ \mathbf{0}]^T \in \mathcal{R}^{(N-1)\times 1},$$
$$C = [h_1\ h_2 \cdots h_{N-1}] \in \mathcal{R}^{1\times(N-1)}, \quad D = h_0.$$

The state-space representation (13) is converted to the z-transform as

$$z\mathbf{E}_{r,pri}(z) = A\mathbf{E}_{r,pri}(z) + BE_r(z),$$
$$E(z) = C\mathbf{E}_{r,pri}(z) + DE_r(z) + V(z), \quad (14)$$

Using the above (14), the SP model in (7) can be rewritten as

$$H_o(z) = C(zI - A)^{-1}B + D. \quad (15)$$

For deriving the innovation process [27], [28] associated with the power spectral factorization of the secondary path, the power spectral density of the secondary path $H_o(z)H_o^T(z)$ is first derived as

$$\begin{bmatrix} C(zI-A)^{-1} & I \end{bmatrix} \begin{bmatrix} Q & S \\ S^T & R \end{bmatrix} \begin{bmatrix} (z^{-1}I - A)^{-T}C^T \\ I \end{bmatrix}, \quad (16)$$

where

$$Q = BB^T, \quad S = BD^T, \; R = DD^T.$$

The equation (16) can be rewritten [29] as

$$\begin{bmatrix} C(zI-A)^{-1} & I \end{bmatrix} \begin{bmatrix} Q + APA^T - P & S + APC^T \\ S^T + CPA^T & R + CPC^T \end{bmatrix} \times \begin{bmatrix} (z^{-1}I - A)^{-T}C^T \\ I \end{bmatrix}, \quad (17)$$

For deriving the equation (17) into a spectral factorization form, P satisfying the following conditions is obtained using the Riccati equation solution [30].

$$0 = Q + APA^T - P - (S + APC^T)(R + CPC^T)^{-1} \times (S^T + CPA^T), \quad (18)$$

where P always exist, as A is stable [29].

Using the above (18), the equation (17) can be rewritten as

$$= \{C(zI - A)^{-1}(S + A\bar{P}C^T)(R + C\bar{P}C^T)^{-1} + I\} \times (R + C\bar{P}C^T) \times \{(R+C\bar{P}C^T)^{-1}(S^T+C\bar{P}A^T)(z^{-1}I-A)^{-T}C^T+I\}, \quad (19)$$

where $\bar{P}$ is the maximum value of P.

In the equation (19), the inverse of the first spectral factorization form is defined for the innovation filter $K(z)$ as

$$K(z) = \{C(zI-A)^{-1}(S+A\bar{P}C^T)(R+C\bar{P}C^T)^{-1} + I\}^{-1},$$
$$= I - C\{zI - A + (S+A\bar{P}C^T)(R+C\bar{P}C^T)^{-1}C\}^{-1} \times (S+A\bar{P}C^T)(R+C\bar{P}C^T)^{-1}. \quad (20)$$

$K(z)E(z)$ is a white Gaussian signal $g(z)$ with variance $(R + C\bar{P}C^T)$ and can be defined as

$$g(z) = E(z) - C\{zI - A + (S+A\bar{P}C^T)(R+C\bar{P}C^T)^{-1}C\}^{-1} \times (S+A\bar{P}C^T)(R+C\bar{P}C^T)^{-1}E(z),$$
$$= E(z) - C\hat{\mathbf{E}}_{r,pri}(z). \quad (21)$$

Utilizing the above (21), the estimated *virtual* error signals can be derived as

$$\hat{\mathbf{E}}_{r,pri}(z) = \{zI - A + (S+A\bar{P}C^T)(R+C\bar{P}C^T)^{-1}C\}^{-1} \times (S+A\bar{P}C^T)(R + C\bar{P}C^T)^{-1}E(z). \quad (22)$$

Using the equation (22), the SPI filter can be derived as

$$\hat{\mathbf{e}}_{r,pri}(k+1) = A\hat{\mathbf{e}}_{r,pri}(k) + (S + A\bar{P}C^T)(R + C\bar{P}C^T)^{-1} \times (e_r(k) - C\hat{\mathbf{e}}_{r,pri}(k)), \quad (23)$$

where

$$\hat{\mathbf{e}}_{r,pri}(k+1) = \left[\hat{e}_r(k)\ \hat{e}_r(k-1) \cdots \hat{e}_r(k-N+2)\right]^T \in \mathcal{R}^{(N-1)\times 1}.$$

The *virtual* error signals $\hat{e}_r(k)$ in each iteration can be obtained as

$$\hat{e}_r(k) = \hat{\mathbf{e}}_{r,pri(1)}(k+1), \quad (24)$$

where $\hat{\mathbf{e}}_{r,pri(1)}$ is the first entry of the vector $\hat{\mathbf{e}}_{r,pri}$. The estimated *virtual* desired signals corresponding to the outputs of the lattice filter just ahead of the secondary path can be derived as

$$\hat{d}_r(k) = y_r(k) + \hat{e}_r(k). \quad (25)$$

A summary of the SPI algorithm is shown in Algorithm 2.

B. LATTICE-ORDER DECISION ALGORITHM

The LOD algorithm is proposed to operate the ANC system without knowing the tap length of the optimal FIR filter. The LOD algorithm is performed by using the *virtual* desired signal and the $(M_e + 1)$th estimation error signal, which are the initial and final estimation errors of the lattice filter. The recursion of the estimation errors $\epsilon_m(k)$ is defined as

$$\epsilon_{m+1}(k) = \epsilon_m(k-1) - \kappa_m(k-1)b_m(k), \quad (26)$$

where $m = 0, 1, \ldots, M_e$. Starting with one order, the LOD algorithm increases the lattice order until the average of the final estimation error is less than the average of the initial estimation error by a certain threshold. The average of the estimation errors can be easily estimated using moving averages as

$$\hat{\epsilon}_0(k) = (1-\xi)|\hat{\epsilon}_0(k-1)| + \xi|\epsilon_0(k)|, \quad (27)$$
$$\hat{\epsilon}_{M_e+1}(k) = (1-\xi)|\hat{\epsilon}_{M_e+1}(k-1)| + \xi|\epsilon_{M_e+1}(k)|, \quad (28)$$

where $\epsilon_0(k) = \hat{d}_r(k)$. ξ is set to $1/L$ and L is the interval to update the lattice order, which affects computing memory and the performance of the ANC system.

In this study, to analyze the performance of the LOD algorithm according to L, an excess ratio of the lattice-order (ERLO) is defined as

$$\text{ERLO}(\%) = \left(\frac{M_e - M}{M}\right) \times 100, \quad (29)$$

where M is the tap length of the optimal FIR filter and M_e is the order of the lattice filter estimated using the LOD algorithm.

The LOD algorithm compares the initial estimation error $\hat{\epsilon}_0(k)$, and the final estimation error $\hat{\epsilon}_{M_e+1}(k)$ at each interval and then increases the order of the lattice filter if the ratio

Algorithm 2 Secondary-Path Innovation Algorithm

Require: SP model as the FIR filter $H_o(z) = h_0 + h_1 z^{-1} + h_2 z^{-2} + \cdots + h_{N-1} z^{-N+1}$, Error signals $e(k)$

1) $A = \begin{bmatrix} \mathbf{0} & 0 \\ \mathbf{I} & 0 \end{bmatrix} \in \mathcal{R}^{(N-1)\times(N-1)}$, $B = [1\ \ \mathbf{0}]^T \in \mathcal{R}^{(N-1)\times 1}$, $C = [h_1\ h_2 \cdots h_{N-1}] \in \mathcal{R}^{1\times(N-1)}$, $D = h_0$.
2) $Q = BB^T$, $S = BD^T$, $R = DD^T$
3) Find $\bar{P} \in \mathcal{R}^{(N-1)\times(N-1)}$ satisfying $0 = Q + A\bar{P}A^T - \bar{P} - (S + A\bar{P}C^T)(R + C\bar{P}C^T)^{-1}(S^T + C\bar{P}A^T)$
4) For $k = 1$:end
5) $\quad \hat{\mathbf{e}}_{r,pri}(k+1) = A\hat{\mathbf{e}}_{r,pri}(k) + (S + A\bar{P}C^T)(R + C\bar{P}C^T)^{-1}(e(k) - C\hat{\mathbf{e}}_{r,pri}(k))$
6) $\quad \hat{e}_r(k) = \hat{\mathbf{e}}_{r,pri(1)}(k+1)$, (where $\hat{\mathbf{e}}_{r,pri(1)}(k+1)$ is the first entry of the vector $\hat{\mathbf{e}}_{r,pri}(k+1)$)
7) $\quad \hat{d}_r(k) = y_r(k) + \hat{e}_r(k)$
8) end

TABLE 1. Analysis of ERLO, convergence rate, and steady-state error level according to L ($M = 100$, $\alpha = 3.1$, SNR = 45dB, input signals were white Gaussian noise).

L	5	10	15	20	25	30	35	40
$ERLO$	31.6%	14.1%	13.3%	51.3%	402.6%	450%	378%	325%
Sampling time to reach steady state (Convergence rate)	920	1040	1080	1160	1510	2050	2250	2300
Steady-state error level (dB)	-24.5	-21.5	-19.8	-18.1	-17.0	-16.7	-15.6	-15.1

Algorithm 3 Lattice-Order Decision Algorithm

Initial conditions: $M_e = 1$, $\hat{\epsilon}_m(0) = 0$, $L = constant$, $\xi = 1/L$, $p = 1$, $\alpha = constant$

1) For $k = 1 : end$
2) $\quad \hat{\epsilon}_0(k) = (1-\xi)|\hat{\epsilon}_0(k-1)| + \xi|\epsilon_0(k)|$
3) $\quad \hat{\epsilon}_{M_e+1}(k) = (1-\xi)|\hat{\epsilon}_{M_e+1}(k-1)| + \xi|\epsilon_{M_e+1}(k)|$
4) $\quad$ If $k = p * L$
5) $\quad\quad$ If $\log\left(\frac{|\hat{\epsilon}_0(k)|}{|\hat{\epsilon}_{M_e+1}(k)|}\right) < \alpha$
6) $\quad\quad\quad M_e = M_e + 1$
7) $\quad\quad\quad p = p + 1$
8) $\quad\quad$ end
9) $\quad$ end
10) end

$\hat{\epsilon}_0(k)$ to $\hat{\epsilon}_{M_e+1}(k)$ is not below the threshold α. Specifically, at $k = p * L$, $(p = 1, 2, \cdots)$,

$$M_e \rightarrow M_e + 1 \ \ if \ \ \log\left(\frac{|\hat{\epsilon}_0(k)|}{|\hat{\epsilon}_{M_e+1}(k)|}\right) < \alpha, \qquad (30)$$

where α was set to [2,4] in this study. The α value of 2 indicates that $\hat{\epsilon}_{M_e+1}(k)$ should be reduced by approximately $1/10^2$ of $\hat{\epsilon}_0(k)$. A specific summary of the LOD algorithm is shown in Algorithm 3.

Using white Gaussian noise and correlated signals, the LOD algorithm was tested for various tap lengths of the optimal FIR filter as shown in TABLE 1 and Figs 2 - 4. The LOD algorithm has the following characteristics.

- If the tap length of the optimal FIR filter is long, the LOD algorithm determines the lattice order to be less than the tap length of the optimal FIR filter, providing efficient computing memory and fast convergence rate to the RLSL algorithm.

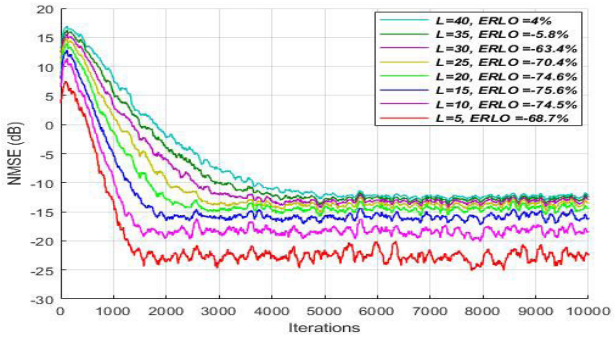

FIGURE 2. NMSE of the RLSL algorithm with the LOD ($M = 500$, $\alpha = 3.4$, SNR = 45dB, input signals were correlated by $G_1(z)$).

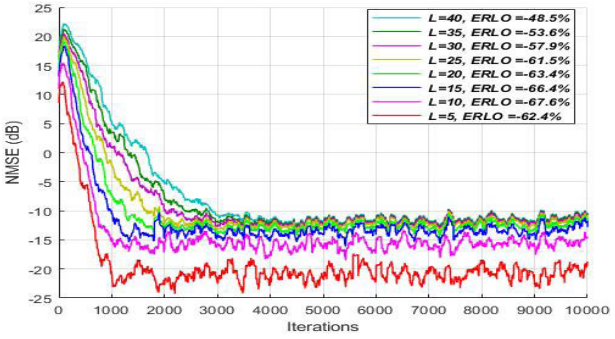

FIGURE 3. NMSE of the RLSL algorithm with the LOD ($M = 300$, $\alpha = 3.4$, SNR = 45dB, input signals were correlated by $G_2(z)$).

- The RLSL algorithm has faster convergence rate and lower steady-state error level as L is smaller. However, if L is less than 5, the LOD algorithm can be unstable since the averages of initial and final estimation errors are changed too quickly.
- ERLO can be large in large L.

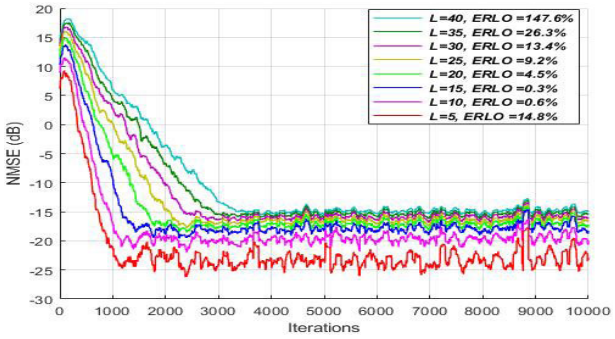

FIGURE 4. NMSE of the RLSL algorithm with the LOD ($M = 100$, $\alpha = 2.8$, SNR = 45dB, input signals were correlated by $G_3(z)$).

Based on the above characteristics, L was set to 5 in this study.

IV. SIMULATION

Simulations were performed in four cases depending on the correlated input signals. All results are presented by averaging 100 independent simulations. The criterion of the performance was set to normalized mean-square error (NMSE), which is defined as

$$\text{NMSE}(k)\ (\text{dB}) = 10\log_{10}\frac{||d(k) - y(k)||^2}{||d(k)||^2}, \qquad (31)$$

where the desired target noises $d(k)$ was set to

$$d(k) = \sum_{n=0}^{N-1} u(k-n)h_n + v(k), \qquad (32)$$

where $u(k)$ is defined as $u(k) = \sum_{i=0}^{M-1} x(k-i)w_i$ and w_i represents the coefficients of the optimal FIR filter $\mathbf{w_o}$ with length of 100 and 300, which are expressed as $W_{o,1}(z)$ and $W_{o,2}(z)$, respectively. h_n represents the coefficients of the SP model $\mathbf{h_o}$. As shown in Fig. 5 and 6, the SP was modeled in four types, generated through polynomial expansion of the pole/zero information using MATLAB, depending on the tap length (50 and 200) and phase (minimum and non-minimum phases). The measurement noise $v(k)$ set to white Gaussian noise was injected according to the signal-to-noises ratio (SNR). The filtered-input NLMS (FxNLMS), FxGAL, and FxRLS algorithms were compared with the proposed RLSL algorithm. The FxNLMS algorithm was chosen, as it is a representative algorithm for adaptive filters. The FxGAL algorithm was chosen to show the difference between the algorithms based on the stochastic gradient approach and the least-square estimation approach. The FxRLS algorithm, which shows the best performance for adaptive filters, was chosen to show that its performance is almost the same as that of the proposed RLSL algorithm with low computational complexity. The computational complexities of each algorithm are shown in TABLE 2.

To evaluate the numerical stability of the comparison algorithms for mismatched SP models, each algorithm were

TABLE 2. Number of multiplication operations per one sample. (M is the tap length of the optimal FIR filter, N is the tap length of the SP model.)

Algorithm	Multiplication	$M = 100$, $N = 50$	$M = 300$, $N = 200$
FxNLMS	$3M + N$	350	1100
FxGAL	$21M + 2N$	2200	6700
FxRLS	$4M^2 + 4M + 2N$	40500	361600
Proposed RLSL	$23M + 2N - 2$	2198	6498

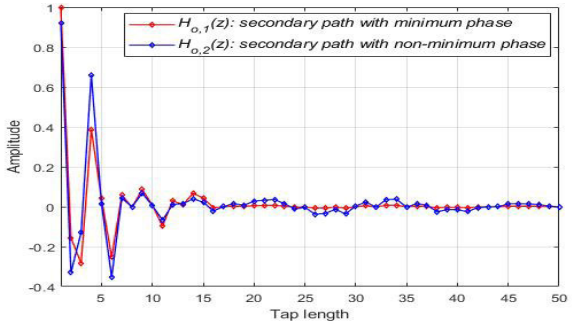

FIGURE 5. SP model with the tap length of 50.

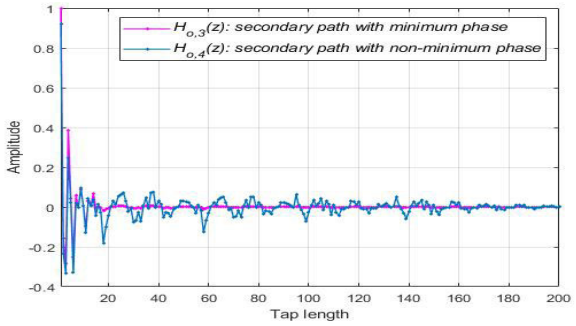

FIGURE 6. SP model with the tap length of 200.

simulated using the mismatched SP models generated by a mismatched degree (MD) of the SP model. The MD of the SP model is defined as

$$\text{MD}(\%) = \frac{\sum_{n=0}^{N-1}(\hat{h}_n - h_n)}{\sum_{n=0}^{N-1} h_n} \times 100, \qquad (33)$$

where $\hat{h}_n$ represents the coefficients of the estimated SP model. As seen in TABLE 3 and 4, the numerical stability is expressed as stable and unstable for each MD of the SP model. If the algorithm is stable, the average of the steady-state error levels is shown, and if the algorithm is unstable, the approximate number of iterations before the algorithm diverges is shown.

All simulations with these comparison algorithms assume that the tap length of the optimal FIR filter is known in advance. If the tap length of the optimal FIR filter is unknown, only the proposed RLSL algorithm with the LOD algorithm is simulated, as the comparison algorithms cannot be performed in the situation.

TABLE 3. Evaluation of the numerical stability of the comparison algorithms for mismatched SP model (SP model: $H_{o,2}(z)$, SNR = 35dB, input signals were correlated by $G_2(z)$).

Algorithm	MD of the SP model (%)							
	70	50	30	10	−10	−30	−50	−70
FxNLMS ($\mu = 0.2$)	Stable, +3.4dB	Stable, +2.5dB	Stable, −0.4dB	Stable, −9.6dB	Stable, −8.8dB	Stable, +1.3dB	Stable, +8.2dB	Stable, +16.8dB
FxGAL ($\mu = 0.005, \lambda = 0.995$)	Stable, −1.5dB	Stable, −3dB	Stable, −5.8dB	Stable, −10.5dB	Stable, −9dB	Stable, −0.8dB	Stable, +7dB	Stable, +15.3dB
FxRLS ($\lambda = 0.995, P_0 = 0.01I$)	Stable, −14.4dB	Stable, −14.3dB	Stable, −13.4dB	Stable, −13.5dB	Stable, −13dB	Stable, −10.9dB	Unstable, 1255 iterations	Unstable, 683 iterations
Proposed RLSL ($\lambda = 0.995$)	Stable, −12.4dB	Stable, −12.7dB	Stable, −12.2dB	Stable, −11.6dB	Stable, −11dB	Stable, −8.8dB	Stable, −8.2dB	Unstable, 5038 iterations
Proposed RLSL with LOD algorithm ($\lambda = 0.995, \alpha = 3.0, L = 5$)	Stable, −11.6dB	Stable, −12.2dB	Stable, −11.4dB	Stable, −10.4dB	Stable, −10.6dB	Stable, −7dB	Stable, −6.1dB	Unstable, 4568 iterations

TABLE 4. Evaluation of the numerical stability of the comparison algorithms for mismatched SP model (SP model: $H_{o,4}(z)$, SNR = 45dB, input signals were correlated by $G_3(z)$).

Algorithm	MD of the SP model (%)					
	50	30	10	−10	−30	−50
FxNLMS ($\mu = 0.2$)	Stable, +0.2dB	Stable, −2.1dB	Stable, −2.4dB	Unstable, 4480 iterations	Unstable, 550 iterations	Unstable, 480 iterations
FxGAL ($\mu = 0.001, \lambda = 0.995$)	Stable, −11.3dB	Stable, −13.8dB	Stable, −15.3dB	Stable, −9.8dB	Stable, −7.3dB	Stable, −2dB
FxRLS ($\lambda = 0.998, P_0 = 0.01I$)	Stable, −22.4dB	Stable, −24.2dB	Stable, −23.2dB	Unstable, 1520 iterations	Unstable, 1090 iterations	Unstable, 683 iterations
Proposed RLSL ($\lambda = 0.995$)	Stable, −21.9dB	Stable, −23.7dB	Stable, −22dB	Stable, −21.4dB	Stable, −16.8dB	Stable, −9.6dB
Proposed RLSL with LOD algorithm ($\lambda = 0.995, \alpha = 3.0, L = 5$)	Stable, −17dB	Stable, −22.6dB	Stable, −19.9dB	Stable, −13.3dB	Stable, −10.6dB	Stable, −8.6dB

A. CASE 1

The first simulation for the SNR of 45dB used the correlated inputs obtained from passing white Gaussian noise through the succeeding filters as

$$G_1(z) = \frac{1+0.9z^{-1}+0.6z^{-2}+0.81z^{-3}-0.329z^{-4}}{1-0.9z^{-1}}.$$

First, the optimal FIR filter and the SP were modeled to $W_{o,1}(z)$ and $H_{o,1}(z)$. In the proposed RLSL algorithm, λ and α were set to 0.995 and 3.1, respectively. L was set to 5 and the ERLO was approximately 13.3%. In the FxRLS algorithm, λ was set to 0.995 and P_0 was set to $0.01I$. In the FxGAL algorithm, μ and λ were set to 0.005 and 0.995, respectively. In the FxNLMS algorithm, μ was set to 0.2.

Second, the optimal FIR filter and the SP were modeled to $W_{o,2}(z)$ and $H_{o,3}(z)$. In the proposed RLSL algorithm, λ and α were set to 0.995 and 3.1, respectively. L was set to 5 and the ERLO was approximately -41%. In the FxRLS algorithm, λ was set to 0.997 and P_0 was set to $0.05I$. In the FxGAL algorithm, μ and λ were set to 0.005 and 0.995, respectively. In the FxNLMS algorithm, μ was set to 0.7.

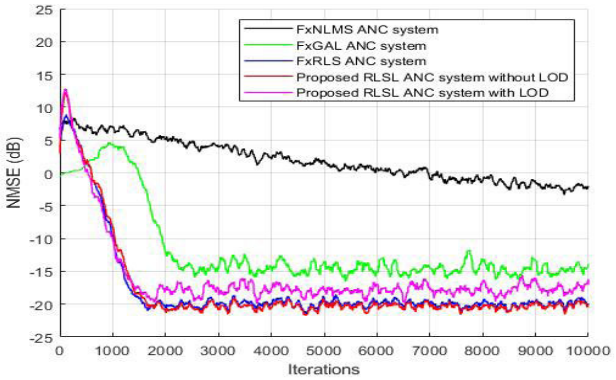

FIGURE 7. NMSE in case 1 ($W_{o,1}(z)$, $H_{o,1}(z)$).

B. CASE 2

The second simulation for the SNR of 35dB used the correlated inputs obtained from passing white Gaussian noise through the succeeding filters as

$$G_2(z) = \frac{1+0.5z^{-1}+0.81z^{-2}}{1-0.59z^{-1}+0.4z^{-2}}.$$

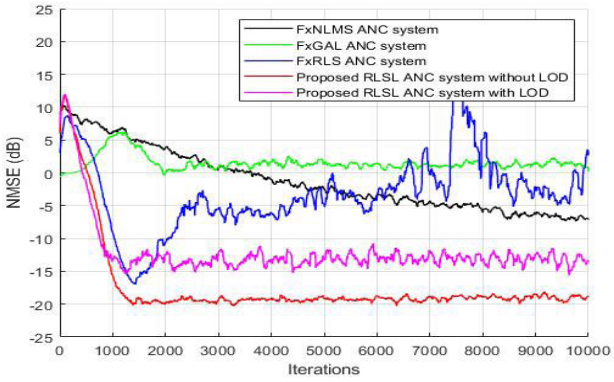

FIGURE 8. NMSE in case 1 when the SP model is mismatched (MD = −50, $W_{o,1}(z)$, $H_{o,1}(z)$).

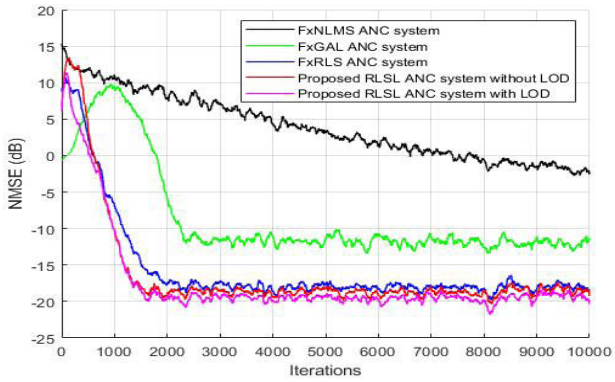

FIGURE 9. NMSE in case 1 ($W_{o,2}(z)$, $H_{o,3}(z)$).

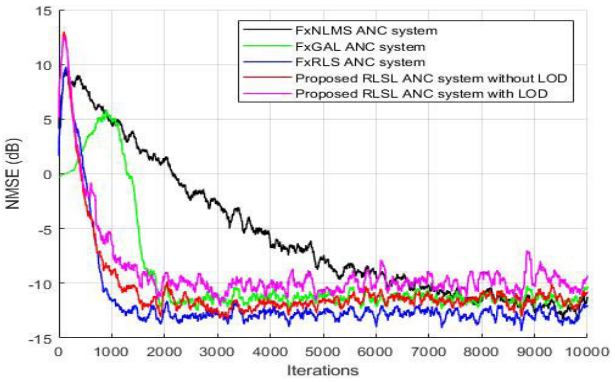

FIGURE 10. NMSE in case 2 ($W_{o,1}(z)$, $H_{o,2}(z)$).

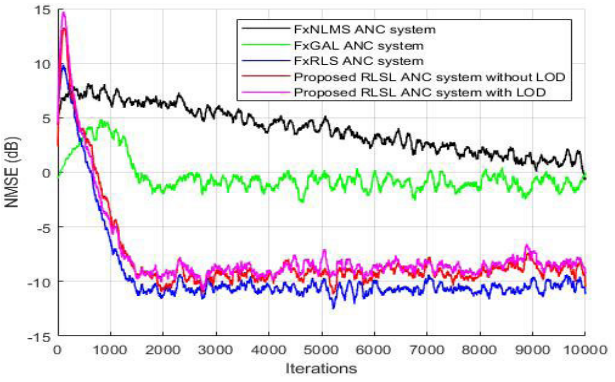

FIGURE 11. NMSE in case 2 when the SP model is mismatched (MD = 50, $W_{o,1}(z)$, $H_{o,2}(z)$).

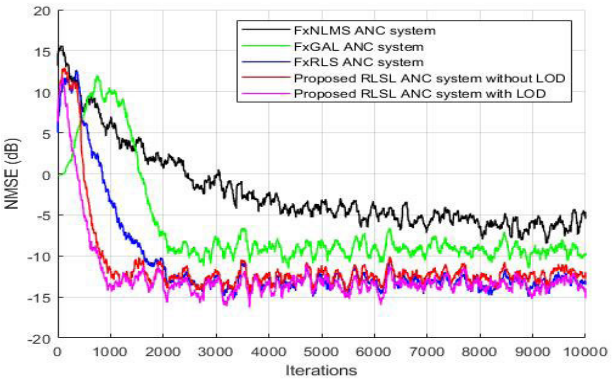

FIGURE 12. NMSE in case 2 ($W_{o,2}(z)$, $H_{o,3}(z)$).

The optimal FIR filter and the SP were modeled to $W_{o,1}(z)$ and $H_{o,2}(z)$. In the proposed RLSL algorithm, λ and α were set to 0.995 and 3.2, respectively. L was set to 5 and the ERLO was approximately 42.7%. In the FxRLS algorithm, λ was set to 0.995 and P_0 was set to $0.01I$. In the FxGAL algorithm, μ and λ were set to 0.005 and 0.995, respectively. In the FxNLMS algorithm, μ, was set to 0.2.

Second, the optimal FIR filter and the SP were modeled to $W_{o,2}(z)$ and $H_{o,3}(z)$. In the proposed RLSL, λ and α were set to 0.995 and 3.1, respectively. algorithm. L was set to 5 and the ERLO was approximately -59.8%. In the FxRLS algorithm, λ was set to 0.998 and P_0 was set to $0.02I$. In the FxGAL algorithm, μ and λ were set to 0.005 and 0.995, respectively. In the FxNLMS algorithm, μ was set to 0.7.

C. CASE 3

The third simulation for the SNR of 45dB used the correlated inputs obtained from passing white Gaussian noise through the succeeding filters as

$$G_3(z) = \frac{1}{1 - 0.9z^{-1}}$$

The optimal FIR filter and the SP were modeled to $W_{o,1}(z)$ and $H_{o,1}(z)$. In the proposed RLSL algorithm, λ and α were set to 0.995 and 3.1, respectively. L was set to 5 and the ERLO was approximately 60.1%. In the FxRLS algorithm, λ was set to 0.995 and P_0 was set to $0.01I$. In the FxGAL algorithm, μ and λ were set to 0.01 and 0.995, respectively. In the FxNLMS algorithm, μ, was set to 0.3.

Second, the optimal FIR filter and the SP were modeled to $W_{o,2}(z)$ and $H_{o,4}(z)$. In the proposed RLSL algorithm, λ and α were set to 0.995 and 3.1, respectively. L was set to 5 and the ERLO was approximately −51.7%. In the FxRLS

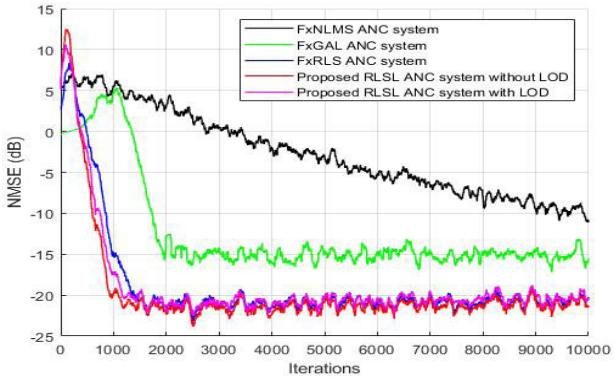

FIGURE 13. NMSE in case 3 ($W_{o,1}(z)$, $H_{o,1}(z)$).

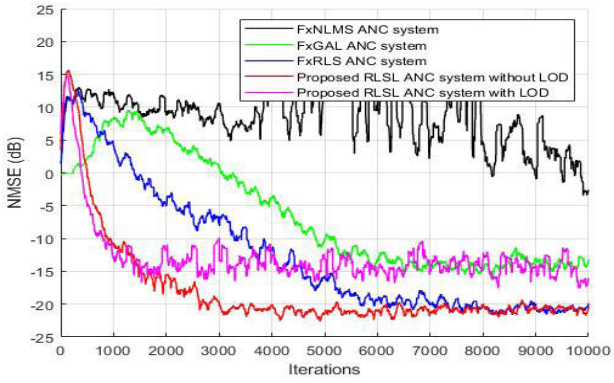

FIGURE 14. NMSE in case 3 ($W_{o,2}(z)$, $H_{o,4}(z)$).

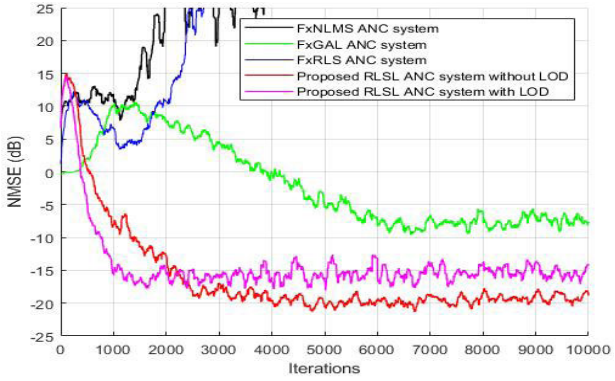

FIGURE 15. NMSE in case 3 when the SP model is mismatched (MD = −30, $W_{o,2}(z)$, $H_{o,4}(z)$).

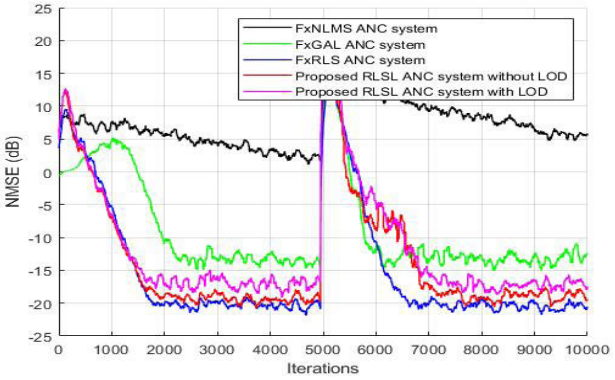

FIGURE 16. NMSE in case 4 ($W_{o,1}(z)$, $H_{o,2}(z)$).

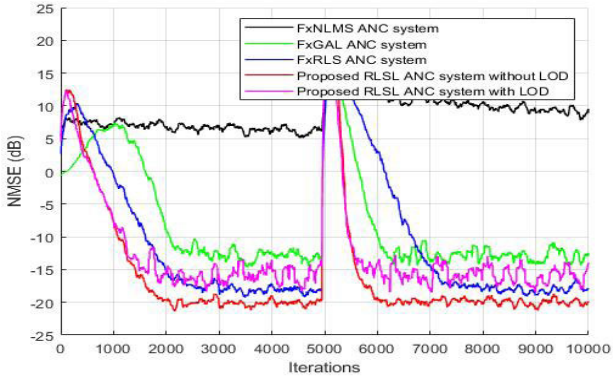

FIGURE 17. NMSE in case 4, ($W_{o,2}(z)$, $H_{o,3}(z)$).

algorithm, λ was set to 0.998 and P_0 was set to $0.01I$. In the FxGAL algorithm, μ and λ were set to 0.001 and 0.995, respectively. In the FxNLMS algorithm, μ was set to 0.2.

D. CASE 4

The final simulations for the SNR of 45dB were performed in the environments where the sign of the optimal FIR filter is suddenly changed. The correlated inputs were set to those as the case 1. The SP model was set to $H_{0,2}(z)$ and $H_{0,3}(z)$.

In case of the SP model with the non-minimum phase $H_{0,2}(z)$, λ and α were set to 0.996 and 3.4, respectively, in the proposed RLSL algorithm. L was set to 5 and the ERLO was approximately 39%. In the FxRLS algorithm, λ was set to 0.996 and P_0 was set to $0.01I$. In the FxGAL algorithm, μ and λ were set to 0.005 and 0.995, respectively. In the FxNLMS algorithm, μ, was set to 0.2.

In case of the SP model with the minimum phase $H_{0,3}(z)$, λ and α were set to 0.996 and 3.5, respectively, in the proposed RLSL algorithm. L was set to 5 and the ERLO was approximately -34.2%. In the FxRLS algorithm, λ was set to 0.997 and P_0 was set to $0.01I$. In the FxGAL algorithm, μ and λ were set to 0.005 and 0.995, respectively. In the FxNLMS algorithm, μ, was set to 0.2.

E. SIMULATION RESULTS

The proposed RLSL algorithm, which has lower computational complexity than the FxRLS algorithm, performed very well for the correlated inputs. The FxGAL algorithm showed a fast convergence rate for the correlated inputs, but was inferior to the proposed RLSL algorithm in terms of the steady-state error level as shown in Fig 7 and 13.

Additionally, for long tap length of the optimal FIR filter, the performance of the FxRLS algorithm was degraded in terms of the convergence rate, but the performance of

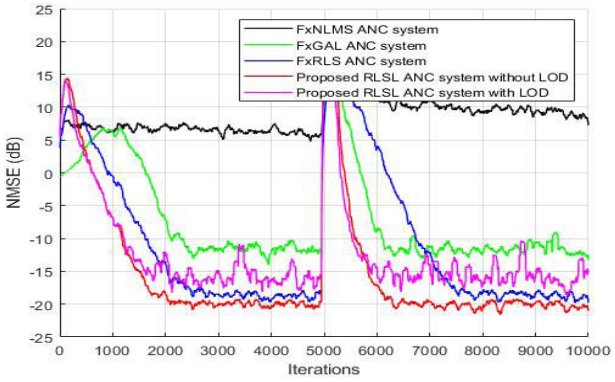

FIGURE 18. NMSE in case 4 when the SP model is mismatched (MD = 10, $W_{o,2}(z)$, $H_{o,3}(z)$).

the proposed RLSL algorithm was very well maintained as shown in Fig 12, 14 and 17. The performance of the proposed algorithm was also robust against unexpected environmental variations as shown in Fig. 16,17 and 18.

For the mismatched SP models, the FxGAL algorithm was always numerically stable, but its performance deteriorated. The FxRLS algorithm performed well when it was numerically stable, but the algorithm was numerically unstable compared to the proposed RLSL algorithm as seen in TABLE 3 and 4. The proposed RLSL algorithm was found to be numerically stable, except for an extreme value of MD $= -70$ in TABLE 3, and to maintain a low steady-state error levels.

Even in environments where the tap length of the optimal FIR filter was not known in advance, only the proposed RLSL algorithm with the LOD algorithm maintained a good performance and numerical stability, which is important to implement the ANC system in real environments.

V. CONCLUSION

Combined with the SPI and LOD algorithms, the RLSL algorithm was applied to the ANC system without the filtered-input structure. For constructing *virtual* desired signals corresponding to the outputs of the lattice filter just ahead of the secondary path, the SPI algorithm associated with the power spectral factorization of the secondary path whitens the error microphone signals passing through the secondary path into the *virtual* error signals just ahead of the secondary path. The LOD algorithm allows the ANC system to maintain its noise reduction performance without knowing the tap length of the optimal FIR filter. The proposed SPI and LOD algorithms can be easily applied to various ANC systems to improve the adaptive filter. The proposed ANC system based on the RLSL algorithm has not only a fast convergence rate and a low steady state error like the ANC system based on the FxRLS algorithm, but also low computational complexity.

REFERENCES

[1] L. Lu and H. Zhao, "Active impulsive noise control using maximum correntropy with adaptive kernel size," *Mech. Syst. Signal Process.*, vol. 87, pp. 180–191, Mar. 2017.

[2] S. Gaur, V. Gupta, "A review on filtered-X LMS algorithm," *Int. J. Signal Process. Syst.*, vol. 4, no. 2, pp. 172–176, 2016.

[3] O. Tobias, J. Bermudez, and N. Bershad, "Mean weight behavior of the filtered-X LMS algorithm," *IEEE Trans. Signal Process.*, vol. 48, no. 4, pp. 1061–1075, Apr. 2000.

[4] M. Akhtar, M. Abe, and M. Kawamata, "A new variable step size LMS algorithm-based method for improved online secondary path modeling in active noise control systems," *IEEE Trans. Audio Speech Lang. Process.*, vol. 14, no. 2, pp. 720–726, Mar. 2006.

[5] D.-C. Chang and F.-T. Chu, "Feedforward active noise control with a new variable tap-length and step-size filtered-X LMS algorithm," *IEEE/ACM Trans. Audio Speech Lang. Process.*, vol. 22, no. 2, pp. 542–555, Feb. 2014.

[6] B. Huang, Y. Xiao, J. Sun, and G. Wei, "A variable step-size FXLMS algorithm for narrowband active noise control," *IEEE Trans. Audio Speech Lang. Process.*, vol. 21, no. 2, pp. 301–312, Feb. 2013.

[7] J. Dhiman, S. Ahmad, and K. Gulia, "Comparison between Adaptive filter Algorithms (LMS, NLMS and RLS)," *Int. J. Sci., Eng. Technol. Res.*, vol. 2, no. 5, pp. 1100–1103, 2013.

[8] S. Douglas, "The fast affine projection algorithm for active noise control," in *Proc. Conf. Rec. 29th Asilomar Conf. Signals, Syst. Comput.*, vol. 2, Nov. 2002, pp. 1245–1249.

[9] A. Carini and G. L. Sicuranza, "Optimal regularization parameter of the multichannel filtered-X affine projection algorithm," *IEEE Trans. Signal Process.*, vol. 55, no. 10, pp. 4882–4895, Oct. 2007.

[10] J.-M. Song and P. Park, "An optimal variable step-size affine projection algorithm for the modified filtered-x active noise control," *Signal Process.*, vol. 114, pp. 100–111, Sep. 2015.

[11] Y. C. Park and S. D. Sommerfeldt, "A fast adaptive noise control algorithm based on the lattice structure," *Appl. Acoust.*, vol. 47, no. 1, pp. 1–25, 1996.

[12] S.-W. Kim, Y.-C. Park, and D.-H. Youn, "A variable step-size filtered-x gradient adaptive lattice algorithm for active noise control," in *Proc. IEEE Int. Conf. Acoust., Speech Signal Process. (ICASSP)*, Mar. 2012, pp. 189–192.

[13] S.-J. Chen and J. Gibson, "Feedforward adaptive noise control with multivariable gradient lattice filters," *IEEE Trans. Signal Process.*, vol. 49, no. 3, pp. 511–520, Mar. 2001.

[14] S. Veena and S. Narasimhan, "Improved active noise control performance based on Laguerre lattice," *Signal Process.*, vol. 84, no. 4, pp. 695–707, Apr. 2004.

[15] S. Veena and S. Narasimhan, "Laguerre escalator lattice and feedforward/feedback active noise control," *Signal Process.*, vol. 87, no. 4, pp. 725–738, Apr. 2007.

[16] J. Lu, C. Shen, X. Qiu, and B. Xu, "Lattice form adaptive infinite impulse response filtering algorithm for active noise control," *J. Acoust. Soc. Amer.*, vol. 113, no. 1, pp. 327–335, Jan. 2003.

[17] S. Kuo and J. Luan, "Cross-coupled filtered-X LMS algorithm and lattice structure for active noise control systems," in *Proc. IEEE Int. Symp. Circuits Syst.*, Dec. 2002, pp. 459–462.

[18] L. Ferdouse, N. Akhter, T. H. Nipa, and F. T. Jaigirdar, "Simulation and performance analysis of adaptive filtering algorithms in noise cancellation," 2011, *arXiv:1104.1962*. [Online]. Available: https://arxiv.org/abs/1104.1962

[19] A. Zeb, A. Mirza, Q. U. Khan, and S. A. Sheikh, "Improving performance of FxRLS algorithm for active noise control of impulsive noise," *Appl. Acoust.*, vol. 116, pp. 364–374, Jan. 2017.

[20] Y. Xiao, L. Ma, K. Khorasani, A. Ikuta, and L. Xu, "A filtered-X RLS based narrowband active noise control system in the presence of frequency mismatch," in *Proc. IEEE Int. Symp. Circuits Syst.*, Jul. 2005, pp. 260–263.

[21] L. Wu, X. Qiu, I. S. Burnett, and Y. Guo, "A recursive least square algorithm for active control of mixed noise," *J. Sound Vibrat.*, vol. 339, pp. 1–10, Mar. 2015.

[22] R. M. Reddy, I. M. S. Panahi, R. Briggs, and E. Perez, "Performance comparison of FXRLS, FXAPA and FXLMS active noise cancellation algorithms on an FMRI bore test-bed," in *Proc. IEEE Dallas Eng. Med. Biol. Workshop*, Nov. 2007, pp. 130–133.

[23] M. Shensa, "Recursive least squares lattice algorithms–A geometrical approach," *IEEE Trans. Autom. Control.*, vol. 26, no. 3, pp. 695–702, Jun. 1981.

[24] D. Lee, M. Morf, and B. Friedlander, "Recursive least squares ladder estimation algorithms," *IEEE Trans. Circuits Syst.*, vol. 28, no. 6, pp. 467–481, Jun. 1981.

[25] H. Sano, S. Adachi, and H. Kasuya, "Application of least squares lattice algorithm to active noise control for automobile," in *Proc. Amer. Control Conf. (ACC)*, vol. 1, Aug. 2005, pp. 821–825.
[26] S. Haykin, *Adaptive Filter Theory*, 2nd ed. Upper Saddle River, NJ, USA: Prentice-Hall, 1991.
[27] T. Lacey, "Tutorial: The Kalman filter," Georgia Inst. Technol., Atlanta, GA, USA, 2019.
[28] S.-M. Guo, L. S. Shieh, G. Chen, and N. P. Coleman, "Observer-type Kalman innovation filter for uncertain linear systems," *IEEE Trans. Aerosp. Electron. Syst.*, vol. 37, no. 4, pp. 1406–1418, Oct. 2001.
[29] B. D. Anderson, J. B. Moore, *Optimal Control: Linear Quadratic Methods*. Chelmsford, MA, USA: Courier Corporation, 2007.
[30] S. Bittanti, A. J. Laub, and J. C. Willems, *The Riccati Equation*. Berlin, Germany: Springer, 2012.
[31] M. Bouchard, "Recursive least-squares algorithms with good numerical stability and constrained least-squares algorithms for multichannel active noise control or transaural sound reproduction systems," in *Proc. IEEE Trans. Speech Audio Process.*, Mar. 2001.
[32] M. Bouchard, "Numerically stable fast convergence least-squares algorithms for multichannel active sound cancellation systems and sound deconvolution systems," *Signal Process.*, vol. 82, no. 5, pp. 721–736, May 2002.
[33] P. Regalia, "Numerical stability properties of a QR-based fast least squares algorithm," *IEEE Trans. Signal Process.*, vol. 41, no. 6, pp. 2096–2109, Jun. 1993.
[34] P. A. Regalia, "Numerical stability issues in fast least-squares adaptation algorithms," *Opt. Eng.*, vol. 31, no. 6, pp. 1144–1153, 1992.

DONG WOO KIM received the B.S. and M.S. degrees in electronic and electrical engineering from the Pohang University of Science and Technology, Pohang, South Korea, in 2014 and 2016, respectively, where he is currently pursuing the Ph.D. degree in electronic and electrical engineering. His research interests include adaptive filtering algorithm and active noise control systems.

POOGYEON PARK (Member, IEEE) received the B.S. and M.S. degrees in control and instrumentation engineering from Seoul National University, Seoul, South Korea, in 1988 and 1990, respectively, and the Ph.D. degree from Stanford University, Stanford, CA, USA, in 1995.

From 1996 to 2000, he was an Assistant Professor with the Pohang University of Science and Technology. Since 2006, he has been a Professor with the Electronic Electrical Engineering Department, Pohang University of Science and Technology. He has authored over 170 articles and the total citation for his articles is 9712. His research interest includes control and signal processing.